Heterogeneities and strain glass behavior: Role of nanoscale precipitates in low-temperature-aged $Ti_{48.7}Ni_{51.3}$ alloys

Yuanchao Ji,[1,2,*] Xiangdong Ding,[1,3] Turab Lookman,[3] Kazuhiro Otsuka,[2] and Xiaobing Ren[1,2,†]

[1]*Multi-Disciplinary Materials Research Center, Frontier Institute of Science and Technology, and State Key Laboratory for Mechanical Behavior of Materials, Xi'an Jiaotong University, Xi'an 710049, People's Republic of China*

[2]*Ferroic Physics Group, National Institute for Materials Science, Tsukuba, 305-0047, Ibaraki, Japan*

[3]*Theoretical division, Los Alamos National Laboratory, Los Alamos, New Mexico 87545, USA*

(Received 16 November 2012; published 22 March 2013)

A frozen short-range, strain-ordered state has been observed in several doped ferroelastic/martensitic alloys. The reported strain glass behavior has been attributed to atomic-scale point defects such as dopant atoms. We report here how nanoscale precipitates can also lead to such glassy behavior. Nanosized, randomly distributed Ti_3Ni_4-like precipitates, produced by aging/annealing at 473 K for 3 h, prohibit the B2 → B19′ martensitic transition that occurs in a precipitate-free state. The strain glass transition is characterized by a mechanical susceptibility/modulus anomaly with Vogel-Fulcher type frequency-dependence, ergodicity-breaking, invariance in average structure and nanosized strain domains. Our work emphasizes that heterogeneities or in general disordering effects in ferroelastics will also give rise to signatures characteristic of strain glass behavior.

DOI: 10.1103/PhysRevB.87.104110 PACS number(s): 64.70.K−, 81.30.Kf, 64.60.Cn

I. INTRODUCTION

Glass, an intriguing phenomenon, has been observed in a wide range of complex systems and yet its nature is not completely understood.[1] Recently, a glassy state, strain glass, has been observed in a number of ferroelastic/martensitic materials.[2–6] This state may be considered an analog of ferroelectric relaxor in ferroelectric materials[7,8] and cluster-spin glass in ferromagnetic materials.[9,10] This observation opens a potential vista for interesting applications, such as the unexpected shape memory effect and superelasticity of the "nonmartensitic" system,[4] as well as stress tuned damping properties.[6] The strain glass is ascribed to the freezing of local lattice strain due to randomly distributed point defects (excess solute atoms or foreign alloying dopants) which prohibit the formation of long-range strain-ordered martensite.[11] Such a role of point defects and disorder on the transition behavior has been discussed theoretically by discrete models of ferroelastics using Monte Carlo methods and the tools of statistical mechanics, as well as phase field simulations.[12]

However, the strain glass experiments reported so far have exclusively focused on the impact of point defects due to doping of the alloys. These defects may be considered as zero-dimensional defects.[13] However, there seems no reason to ignore the possibility that the glassy behavior can also be caused by other crystallographic defects such as dislocations (one-dimensional defects) or nanoparticles (three-dimensional defects), which also suppress phase transitions in martensitic systems.[14–19] Here we report an example of a strain glass caused by nanosized particles. This glass will possess not only the unique properties of giant low hysteresis previously observed in strain glass, but also the enhancement of mechanical properties by particle hardening. Our work leads to "the second route" to yield strain glass and deviate the transition path, which may bring some surprising physical properties.

II. EXPERIMENTAL TECHNIQUE

It is well known that in Ni-rich Ti-Ni alloys, the Ti_3Ni_4 precipitates produced by aging/annealing can significantly change the behavior of the martensitic transition.[15–19] Nanosized precipitates have been observed if the sample is aged at very low temperatures, such as 473 K.[18,20] In addition, when aging at low temperatures, the precipitates can be more homogeneously distributed across the whole sample, especially in Ni-rich TiNi alloys.[17] In this work, nanosized precipitates were obtained at the early state of low temperature aging in Ni-rich TiNi alloys. The experimental samples were cut from the $Ti_{48.7}Ni_{51.3}$ polycrystals (supplied by Furukawa Electric Co. Ltd.), and solution treated at 1273 K for 1 h (with argon atmosphere in quartz tubes containing pure Ti), and then followed by quenching into water. After the solution treatment (precipitate-free state), some of the samples were aged at 473 K for 3 h and quenched into water to get the samples with precipitates. The characterization of the microstructure was performed by high resolution transmission microscope (HREM) using JEM-2100F, recorded using GATAN CCD slow scan camera and analyzed by DigitalMicrograph software. Low temperature observation was done by JEM-2010 microscope with a double tilt liquid helium cooling holder. The transition behavior was studied using differential scanning calorimetry DSC (Q200 TA Instruments) with cooling and heating rate of 10 K/min and electrical resistivity by a four-probe method with a constant current of 100 mA. The x-ray diffraction (XRD7000 Shimadzu) experiment was performed to detect the possible structural change with the temperature. The dynamical mechanical properties were conducted on a dynamic mechanical analyzer DMA (Q800 TA Instruments) using step cooling and heating methods with dual cantilever mode in the frequency range from 0.2 Hz to 20 Hz.[5] Zero-field-cooling/field-cooling (ZFC/FC) measurements[3] were also carried on the same DMA machine using film tension mode.

III. EXPERIMENTAL RESULTS

We first characterized the size and distribution of the precipitates in the aged samples. Figure 1(a) reveals that in the aged samples the nanosized precipitates are dispersed and

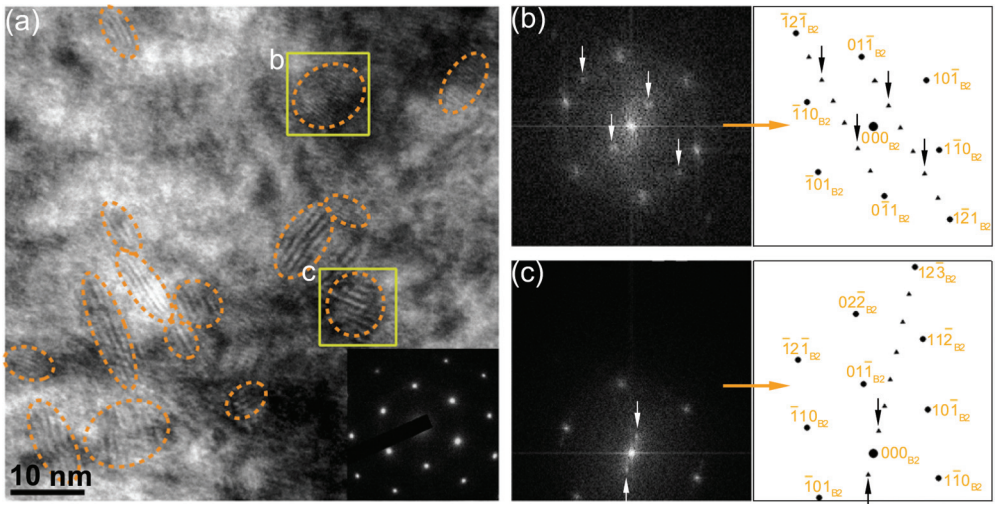

FIG. 1. (Color online) HREM image in $[111]_{B2}$ zone axis of an aged sample at room temperature. (a) Precipitates appear as a moiré pattern. (b), (c) The FFT spectrums of the two selected square areas in (a) and their key diagrams. 1/7 spots (strong ones are marked by arrows) suggests the precipitates are Ti_3Ni_4. The difference in the orientation of 1/7 spots between (b) and (c) indicates that the precipitates at location b and c have different crystallographic orientation.

coherently distributed in the B2 matrix, appearing as Moiré modulations due to the lattice mismatch. Figures 1(b) and 1(c) are the fast Fourier transform (FFT) spectrums of the two square regions containing fine precipitates in Fig. 1(a). The FFT shows additional 1/7 reflections along ⟨123⟩ reciprocal vectors of the B2 type matrix, suggesting that the nanosized precipitates are Ti_3Ni_4.[15,21] Nevertheless, we noticed that the absence of some 1/7 spots indicates the early stage of formation of Ti_3Ni_4 precipitates, which have not developed well at such low temperature at early time, in agreement with previous studies.[18–20]

We then investigated the effect of precipitate on the transition behavior of the samples. First, the DSC measurements [Figs. 2(a) and 2(d)] show that the precipitate-free sample undergoes the B2 → B19′ martensitic transition, appearing as an enthalpy peak/dip in the DSC curves. The hysteresis between the martensite starting temperature and the reverse transition finishing temperature is around 30 K, evidence for the occurrence of a first-order phase transition. However, in the precipitate-bearing sample only a broad hump is observed over the testing temperature range and this suggests a very weak transition, but obviously not the normal martensitic transition. Second, Figs. 2(b) and 2(e) show the temperature spectrum of resistivity. In Fig. 2(b) the B2 → B19′ transition occurs by exhibiting two peaks in the cooling and heating cycles. The temperature difference between the peaks is the hysteresis for the martensitic transition, ∼35 K. However, all of these features disappear in the precipitate-bearing sample, shown in Fig. 2(e). Third, *in situ* XRD measurements [Figs. 2(c) and 2(f)] show that the B19′ martensite has already formed in the precipitate-free sample, proved by an additional diffraction peak at low temperature (due to the temperature limitation of the XRD machine, the diffraction peak of the parent phase does not completely disappear); the precipitate-bearing sample shows almost no change and keeps the B2 structure of the parent phase over the entire temperature range, indicating the absence of a phase transition. All above results demonstrate that the formation of the B19′ phase in the precipitate-bearing sample is inhibited.

Although the above results reveal the absence of a martensitic transition in the precipitate-bearing sample, it does not mean that there is no transition in the precipitate-bearing sample. The additional measurements in the following show that a glass transition occurs in the sample.

As dynamics plays a crucial role in the freezing process of the glassy state, the most common experimental technique is the measurement of the frequency dependence of a relevant dynamic variable (the ac elastic/storage modulus and internal

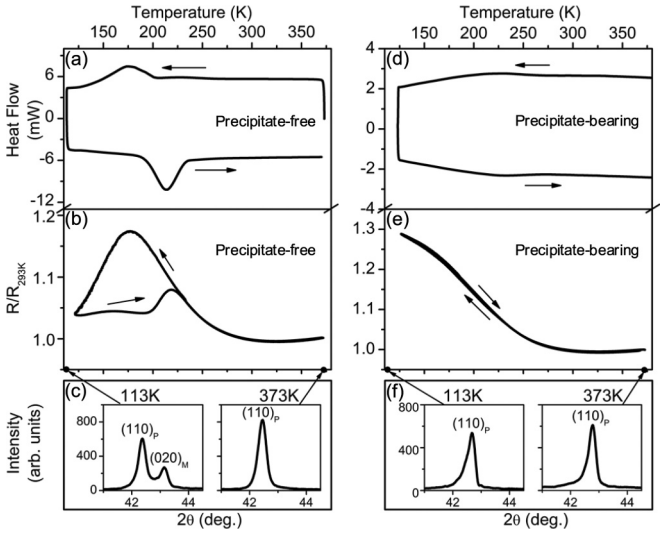

FIG. 2. Transition behaviors of precipitate-free and precipitate-bearing sample. DSC curves [(a) and (d)], resistivity results [(b) and (e)], and *in situ* XRD measurements at different temperature [(c) and (f)] show that normal martensitic transition, present in the precipitate-free sample, is completely suppressed in the precipitate-bearing sample.

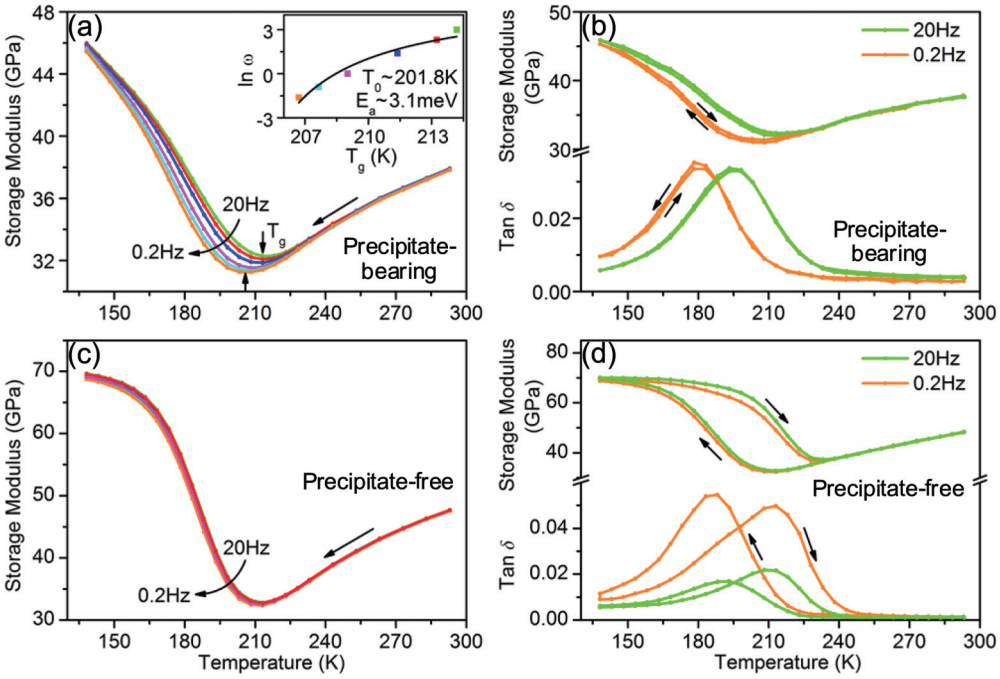

FIG. 3. (Color online) DMA results of precipitate-bearing and precipitate-free sample. (a) Storage modulus exhibits a frequency-dependent dip at $T_g \sim 210$ K with the dip temperature following Vogel-Fulcher relation $\omega = \omega_0 \exp[-E_a/k_B(T_g - T_0)]$ (the inset), where ω is the frequency, ω_0 the frequency prefactor, E_a the activation energy, k_B the Boltzmann constant, T_g the strain glass freezing temperature, and T_0 the ideal freezing temperature. (b) Both storage modulus and internal friction show little hysteresis from low frequency 0.2 Hz to high frequency 20 Hz. (c), (d) Instead, normal martensitic transition is shown by frequency independence of modulus dips and large hysteresis between the cooling and heating process, respectively.

friction for the ferroelastic system). The temperature dependent curves of the storage modulus for the precipitate-bearing sample show dips in Figs. 3(a) and 3(b), suggesting clearly the occurrence of a certain phase transition. However, this transition differs from that of a long-range ordered martensitic transition [Figs. 3(c) and 3(d)]. It exhibits frequency dependence of the dip temperature from 0.2 Hz to 20 Hz. This feature, absent for a long-range ordered phase transition [Fig. 3(c)], is characteristic of a glass transition and has been observed in the various glassy phases (ferroelectric relaxor,[7] spin glass,[1,9] and strain glass[2,5]). The frequency dispersion of storage modulus follows the Vogel-Fulcher relation, shown in the inset of Fig. 3(a). In addition, little hysteresis between the cooling and heating processes can be observed from both the storage modulus and the internal friction curves in Fig. 3(b). This is also a clear difference from that of the normal martensitic transition [Fig. 3(d)].

Another signature for glassiness is the behavior of nonergodicity or history dependence. A well-known experimental method for detecting the nonergodicity is the so-called zero-field-cooling (ZFC)/field-cooling (FC) measurement.[3] In the ZFC process the samples are first cooled to well below T_g under zero stress, then loaded (stress $\sigma = 20$ MPa) and heated up to far above T_g under this stress; in the FC process the samples are cooled with a constant stress (20 MPa) and then heated again at the same stress. The strain responses shown in the ZFC/FC curves are recorded during the heating process. Figure 4 shows that the precipitate-bearing sample behaves as the typical ZFC/FC curve compared with previous studies on various glasses (ferroelectric relaxor,[8] spin glass,[1,10] and strain glass[3]). In contrast to the continuous decrease of the FC curve, the ZFC curve shows a peak at around 198 K, representing the glass transition temperature. The difference in ZFC/FC curves becomes smaller and smaller and coincides at a certain temperature with increasing temperature. The large deviation between the ZFC and FC curves demonstrates the history dependence of the strain state, a direct evidence for broken ergodicity.

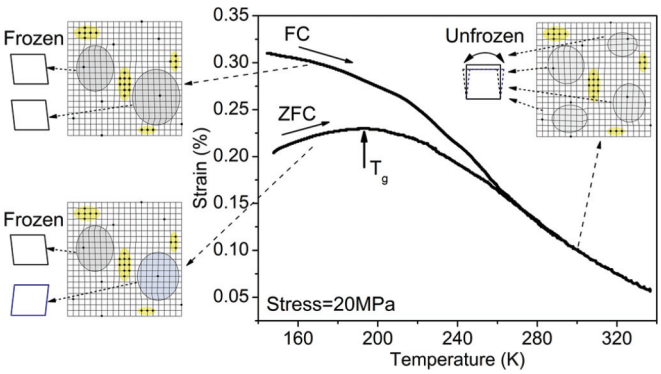

FIG. 4. (Color online) ZFC/FC curves of precipitate-bearing sample show large deviation especially below T_g (~198 K), indicating the history dependence of the strain state, which is schematically depicted by the left panel and the inset figure (different frozen strain states evolving from the same unfrozen one).

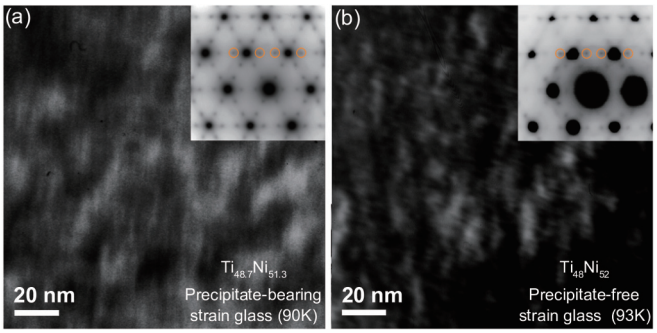

FIG. 5. (Color online) TEM images and associated diffraction patterns of two different strain glass systems. (a) Precipitate-induced strain glass reveals randomly distributed nanosized domains of 20–40 nm; the inset shows incommensurate 1/3 diffuse spots, which are much stronger than that at room temperature [inset of Fig. 1(a)]. (b) Similar features are shared by point-defect-induced strain glass.[2] It should be noted that Ti_3Ni_4 spots in (a) are too weak to be invisible.

To reveal the nature of this precipitate-induced glassy state, low temperature TEM observation [Fig. 5(a)] was performed at 90 K (well below T_g) for a precipitate-bearing sample. It is found that the strain glass is characterized by randomly distributed nanosized strain domains with a size of 20–40 nm. Diffraction pattern shows the existence of diffuse superlattice reflections, appearing at incommensurate positions near $1/3\langle 110\rangle$ of B2 matrix. These features are similar to those found in precipitation-free, point-defect-induced strain glass of Ti-Ni alloys, as shown in Fig. 5(b) (Ref. 2). This suggests that the local strain order is R phase, being the same as that of the point-defect-induced strain glass in Ni-rich Ti-Ni alloys. It should be noted that nanoprecipitates are not clearly seen in Fig. 5(a) due to much reduced TEM resolution using cooling holder.

IV. DISCUSSION

The above results clearly show the existence of a strain glass state in the precipitate-bearing samples. However, the origin of this strain glass is quite different. Previously it was obtained *only* by doping point defects, i.e., the atomic-scale defects lead to the formation of strain glass. The strain glass reported here is not due to the point defects (strain glass transition does not occur in the precipitation-free sample and the concentration of point defects (excess Ni atom) even reduces after aging/annealing), but due to the precipitates upon aging. These huge numbers of randomly distributed nanosized precipitates produce local lattice distortions and lead to a heterogeneous disordered strain state, thereby suppressing the long-range strain-ordering martensitic transition. As a result, the transition behavior transforms from a long-range ordered martensitic state to a short-range ordered glass state, as expected.

It is clear that the precipitate-induced strain glass phase shows qualitatively the same glass features as those found in point-defect induced Ti-Ni strain glass,[2–5] such as the frequency-dispersion in elastic modulus, nonergodicity as reflected by ZFC/FC measurements, invariance of average structure, and the existence of R nanodomains. However, they also have some differences if compared in a quantitative way. First, the precipitate-induced strain glass has higher glass transition temperature ($T_g \sim 210$ K) as compared with that of point-defect-induced strain glass ($T_g \sim 170$ K) in $Ti_{48.5}Ni_{51.5}$ (Ref. 2). Secondly, the former has larger domain size (20–40 nm) than that of the latter (10–20 nm), as shown in Fig. 5. Such quantitative differences suggest a dependence of the glass behavior on the length scale of the precipitates (atomic defect can be viewed as precipitate composed of one atom), and it seem that the larger the precipitates the larger the strain domains are [as seen by comparison between Figs. 5(a) and 5(b)]. Indeed, strain glass transition becomes normal martensitic (R-phase) transition if the precipitates grow into a large size.[15]

The length-scale or precipitate-size dependence of the strain glass transition can be explained by considering the effect of the defect length scale on the randomness. It is known that randomness plays a key role in the formation of strain glass.[12] The random local distortions/fields generated by defects interact with the strain order parameters and break the local symmetry and result in a short-range strain ordered state—strain glass. Both atomic defects/dopants and nanoprecipitates can produce random strain field, but to different extent. Atomic defects are most randomly dispersed in the lattice and thus cause the strongest randomness effect; as a result, the corresponding strain glass has smaller domain size and lower freezing temperature. Nanoprecipitates also produce random strain field and create strain glass, as reported in the present paper; but clearly the extent of the randomness is less than that of the atomic defects/dopants, because the separation of the strain centers between two precipitates is much larger than that between two atomic defects. As a result, the nanoprecipitate-induced strain glass has larger domain size and higher freezing temperature. When the precipitate size is sufficiently large (i.e., after annealing at higher temperature or longer time), the strain randomness is small, because the separation of the precipitates is too large and the strain field between them is largely homogenous. In such a case, instead of local strain freezing (or strain glass) the system undergoes a long-range strain ordering transition—martensitic transformation (R phase transition here); this is a well-known result.[15]

In conclusion, we have demonstrated that the glassy behavior in ferroelastics can be caused by nanosized precipitates. We thus expect other heterogeneities and disordering effects to give rise to a similar glass phase. It will be interesting to determine whether the associated mechanical properties of the phase will be different and how it will depend on the nature of the heterogeneity. Similarly, we speculate that heterogeneities in relaxor ferroelectrics and magnetic systems will have similar effects.

ACKNOWLEDGMENTS

The present work was supported by the following grants: No. 2012CB619401, No. 2010CB631003, No. 51171140, No. 51231008, No. 22360278, and No. 2010628055. We thank S. W. Guo, Z. Zhang, D. Wang, J. H. Gao, S. Yang, Y. Wang, and Y. M. Zhou for technical support and helpful discussion.

*Corresponding author: Ji.Yuanchao@nims.go.jp
†Corresponding author: REN.Xiaobing@nims.go.jp

[1]K. Binder and W. Kob, *Glassy Materials and Disordered Solids: An Introduction to Their Statistical Mechanics* (World Scientific, London, 2005).
[2]S. Sarkar, X. Ren, and K. Otsuka, Phys. Rev. Lett. **95**, 205702 (2005).
[3]Y. Wang, X. Ren, K. Otsuka, and A. Saxena, Phys. Rev. B **76**, 132201 (2007).
[4]Y. Wang, X. Ren, and K. Otsuka, Phys. Rev. Lett. **97**, 225703 (2006).
[5]Y. Zhou, D. Xue, X. Ding, K. Otsuka, J. Sun, and X. Ren, Appl. Phys. Lett. **95**, 151906 (2009); Y. Zhou, D. Xue, X. Ding, Y. Wang, J. Zhang, Z. Zhan, D. Wang, K. Otsuka, and X. Ren, Acta Mater. **58**, 5433 (2010); D. Wang, Z. Zhang, J. Zhang, Y. Zhou, Y. Wang, X. Ding, Y. Wang, and X. Ren, *ibid.* **58**, 6206 (2010); Z. Zhang, Y. Wang, D. Wang, Y. Zhou, K. Otsuka, and X. Ren, Phys. Rev. B **81**, 224102 (2010).
[6]Y. Wang, X. Song, X. Ding, S. Yang, J. Zhang, X. Ren, and K. Otsuka, Appl. Phys. Lett. **99**, 051905 (2011).
[7]L. E. Cross, Ferroelectrics **76**, 241 (1987).
[8]D. Viehland, J. F. Li, S. J. Jang, L. E. Cross, and M. Wuttig, Phys. Rev. B **46**, 8013 (1992).
[9]J. A. Mydosh, *Spin Glasses* (Taylor & Francis, London, 1993).
[10]N. Gayathri, A. K. Raychaudhuri, S. K. Tiwary, R. Gundakaram, A. Arulraj, and C. N. R. Rao, Phys. Rev. B **56**, 1345 (1997).
[11]X. Ren, in *Disorder and Strain-induced Complexity in Functional Materials*, edited by T. Kakeshita, T. Fukuda, A. Saxena, and A. Planes (Springer, Berlin, 2012), Vol. 148.
[12]P. Lloveras, T. Castán, M. Porta, A. Planes, and A. Saxena, Phys. Rev. B **80**, 054107 (2009); R. Vasseur and T. Lookman, *ibid.* **81**, 094107 (2010); D. Wang, Y. Wang, Z. Zhang, and X. Ren, Phys. Rev. Lett. **105**, 205702 (2010); R. Vasseur, D. Xue, Y. Zhou, W. Ettoumi, X. Ding, X. Ren, and T. Lookman, Phys. Rev. B **86**, 184103 (2012).
[13]W. D. Callister, Jr., *Materials Science and Engineering: An Introduction,* 5th ed. (John Wiley & Sons, Inc., New York, 1999).
[14]S. Miyazaki, Y. Igo, and K. Otsuka, Acta Metall. **34**, 2045 (1986).
[15]K. Otsuka and X. Ren, Prog. Mater. Sci. **50**, 511 (2005).
[16]N. Zhou, C. Shen, M. F.-X. Wagner, G. Eggeler, M. J. Mills, and Y. Wang, Acta Mater. **58**, 6685 (2010); W. Guo, I. Steinbach, C. Somsen, and G. Eggeler, *ibid.* **59**, 3287 (2011); S. Cao, M. Nishida, and D. Schryvers, *ibid.* **59**, 1780 (2011).
[17]Y. Zhou, J. Zhang, G. Fan, X. Ding, J. Sun, X. Ren, and K. Otsuka, Acta Mater. **53**, 5365 (2005).
[18]J. I. Kim and S. Miyazaki, Acta Mater. **53**, 4545 (2005).
[19]Y. Zheng, F. Jiang, L. Li, H. Yang, and Y. Liu, Acta Mater. **56**, 736 (2008).
[20]M. Kompatscher, B. Deme, G. Kostorz, Ch. Somsen, and E. F. Wassermann, Acta Mater. **50**, 1581 (2002).
[21]T. Tadaki, Y. Nakata, K. Shimizu, and K. Otsuka, Trans. Jpn. Inst. Met. **27**, 731 (1986).